scientific reports

Check for updates

OPEN

Multi-level trend analysis of extreme climate indices by a novel hybrid method of fuzzy logic and innovative trend analysis

Fereshteh Modaresi[1]✉, Ali Danandeh Mehr[2], Iman Sardarian Bajgiran[1] & Mir Jafar Sadegh Safari[3,4]

Multi-level trend analysis of extreme climate variables is an efficient method for in-depth investigation of the climate change impacts on ecohydrology. However, most of existing statistical methods do not reveal potential trends in different levels of data. In this study, a new approach namely Fuzzy Innovative Trend Analysis (FITA) was introduced that takes the advantages of fuzzy logic to improve and facilitate Innovative Trend Analysis (ITA) abilities to multilevel trend detection at Extreme Climate Indices (ECIs). Regarding the graphical nature of the proposed method, two new indices, namely Grow Percent (GP) and Total Grow Percent (TGP) were suggested for quantifying the power of trend at distinct levels. The FITA was utilized for trend detection at three levels of four important ECIs related to precipitation and temperature. To this end, long-term (1960–2021) daily temperature and precipitation observations at six meteorology stations across diverse climatic zones of Iran were used. The multilevel trends attained by the FITA were further compared to those of ITA, Mann-Kendall (M-K), and Sen's slope (SS) tests. The results indicated that the FITA provides promising results with higher interpretability and reliability than its counterparts at all stations. The underlying high-resolution trends detected at certain stations also pointed out that the M-K and SS tests may yield in misleading interpretations when they are used for identifying trends in ECIs.

Keywords Extreme climate index, FITA, Fuzzy rules, Innovative trend analysis, Grow percent indicator

According to the IPCC Sixth Assessment Report (AR6), the global surface temperature rose by approximately 1.1 °C between 2011 and 2020 compared to the pre-industrial baseline of 1850–1900, underscoring the unequivocal reality of global warming[1]. Regional- and catchment-scale studies have also demonstrated a significant variation of extreme climate variables under climate change[2–4]. Trend analysis is an essential way to assess the impacts of climate change on climate variables. The Expert Team on Climate Change Detection and Indices (ETCCDI) has proposed 27 extreme climate indices (ECIs) to assess extreme climate variation globally and regionally[5,6]. The trends in the extreme indices, which are classified into two groups related to temperature and precipitation, have been assessed in many studies at various regions such as South America[7], Georgia[8], Italy[9], Benin[10], China[11], West Africa[12], Chad[13], Pakistan[14], Brazil[5]India[15]Turkey, [16] and the Middle East[17]. Overall, these studies have shown significant trends in extreme indices, particularly those derived from temperature.

In Iran, long-term variation of ECIs has been explored in a number of studies[18–25]. In line with global studies, significant positive trends in extreme temperatures across the country were reported. The increasing trend in the indices associated with the extreme minimum temperature was more intensive than those of maximum temperature. These studies also demonstrated a decreasing trend in the number of chilly days and nights. In contrast, the number of hot days and nights has been increased markedly[18,22,24–26]. Fathian, et al.[23] revealed that the western, northern, and north western regions of Iran with semi-arid climate were most affected by the risk of climate extremes. Regarding the total annual precipitation, a negative trend for the whole country was reported[18,26] while several studies showed an insignificant trend in the most areas[19,21,22,24]. In addition, significant positive trends in the frequency, intensity, and magnitude of extreme precipitation events, particularly in the south-western Iran along the coast of the Persian Gulf with arid climate were reported[18,19,26,27].

[1]Department of Water Science and Engineering, Faculty of Agriculture, Ferdowsi University of Mashhad, Mashhad, Iran. [2]Civil Engineering Department, Antalya Bilim University, Antalya, Turkey. [3]Department of Geography and Environmental Studies, Toronto Metropolitan University, Toronto, ON, Canada. [4]Department of Civil Engineering, Yaşar University, Izmir, Turkey. ✉email: fmodaresi@um.ac.ir

All these climatic insights were obtained through the well-known conventional Mann-Kendall (M-K), Sen's slope (SS), and linear regression methods. Although climate change alerts trends at different levels of data, these methods are not able to reveal the trends at multiple levels as they evaluate trends merely in the sequential data. Since a special level of extreme events may not occur in a sequential way, their trends could not be detected by the mentioned tests. Moreover, these methods are based on some restrictive assumptions, such as normality and serial independence that are often not met for trend detection in a rather long time series[28]. Therefore, the trend magnitude/slope estimated with these methods may vary significantly for a given ECI[29–31]. To cope with these drawbacks, Şen[32] introduced a new trend analysing method, called Innovative Trend Analysis (ITA), in which potential trends in hydrological time series can be extracted graphically in different levels of data no matter if it is serially correlated or non-normally distributed.

During the past decade, the ITA method has been extensively used in hydro-climatological studies, and its efficiency was compared to the M-K and other conventional trend analysing methods[33–41]. The studies showed that the results of the M-K and ITA are consistent when an overall trend exists in whole dataset. However, when there are different trends in different levels of data like, low, medium, and high, the results of these tests are considerably different from each other. To capture trends by the ITA method in more detail, Zerouali, et al.[42] divided the desired time series into a number of sub-periods (for example, three and four sub-periods for double-ITA and triple-ITA, respectively), and then performed ITA method on each of two consecutive periods (first vs. second, second vs. third, and third vs. forth sub-period). The authors also demonstrated that hidden trends in long-term rainfall time series can better visualized through integration of double-ITA and triple-ITA with Hilbert Huang Transform. Also, a new form of ITA (3D-ITA) was presented for assessing hydrometeorological data[43,44] in which the stability of the trend was evaluated in addition to its existence in data.

Since ITA is a graphical method, assessing the magnitude and significance of the detected trends is a challenging task. Wu and Qian[40] proposed statistic D for quantifying the value of trends identified by ITA for annual rainfall time series. The authors reported that D is comparable with Z value of M-K test. However, the trend analysis of streamflow conducted by Gumus, et al.[34] as well as annual and seasonal rainfall and temperature trend analysis by Cui, et al.[45] showed that D values are much far from the Z-statistic and cannot be interpreted in comparison to Z. Later, Şen[46] suggested another dimensionless statistic, called S, as the slope value of the trend attained via ITA within a given confidence level (CL). The author stated that when the S values are outside of CL the trend is significant. However, it remains unreliable for long nonstationary time series. This was proved in the study of Wang, et al.[41] for trend analysis of annual and seasonal rainfall in the Yangtze River Delta, eastern China. They revealed that although the graphical ITA and M-K tests indicated no significant trend, the S values were identified significantly at the CL of 95%.

Compared to the M-K, SS, and linear regression methods, ITA provides more insight into trends in local minima and maxima[38,47]. However, to the best of the authors' knowledge, the current literature lacks any specific study regarding the efficiency of ITA for multi-level trend analysis of ECI time series. Regarding the extremely non-deterministic nature and unbounded ranges of ECIs, classifying them at multiple classes for trend analysis is an important, albeit more complex, task.

Therefore, this study aimed to present and apply a new approach to facilitate multi-level trend analysis by the ITA method based on an integration of the power of fuzzy logic rules with the graphical feature of the ITA. While the former was used to reduce the level of uncertainties associated with classification thresholds, the graphical element of ITA facilitates visualizing detail trends in multiple classes. The proposed method, called Fuzzy-ITA (hereafter FITA), was demonstrated through analysing four ECI timeseries derived from long-term precipitation and temperature data measured at six meteorology stations distributed in different climatic zones of Iran. To cope with the ITA's problem relevant to quantifying the power of trends, we proposed two indices, namely Grow Percent (GP) and Total Grow Percent (TGP) that reflect the significance of trends detected by the FITA. Unlike S and D, the proposed GP and TGP statistics are perfectly consistent with the results of the graphical test and can be applied for both classified and non-classified hydro-meteorological time series. Eventually, we compared the FITA results with those of M-K, SS, and ITA tests to verify the efficiency of the proposed approach.

Study area and data

Four ECIs, namely annual maximum of maximum temperature (AT_{max}), annual minimum of minimum temperature (AT_{min}), total annual precipitation (APT), and annual precipitation intensity (API) were extracted from 62 years (1960–2021) observed daily temperature and precipitation data at six stations located in diverse climatic zones across Iran. Figure 1 shows the climatic condition of the studied stations based on the de Martonne climate classification, drawn by Arc Map 10.6.1 software. Also, Table 1 summarizes the main geographical information and long-term mean of the ECIs as well as the climatic classification of the studied stations.

As shown in Fig. 1, the country has mostly hyper-arid, arid, and semi-arid climates. A smaller area in the north has climates ranging from the Mediterranean to extremely humid[48]. Table 2 presents the analysed climate indices, while Fig. 2 illustrates their ranges in the respective weather stations. These indices, as defined by ETCCDI, play crucial roles in snow melting, water demand and supply dynamics, and the occurrence of extreme flood events.

Interestingly, Fig. 2 reveals variations in climate indices across stations with similar climate classifications. For instance, stations like Tehran and Mashhad, as well as Esfahan and Kerman, exhibit different ranges in climate indices, particularly those associated with temperature.

Methods

Innovative trend analysis (ITA)

The ITA is a graphical trend analysing method in which a given time series is divided into two equal sub-series, and then, each of the sub-series is sorted in ascending order. The scatter plot of the sub-series is drawn in a

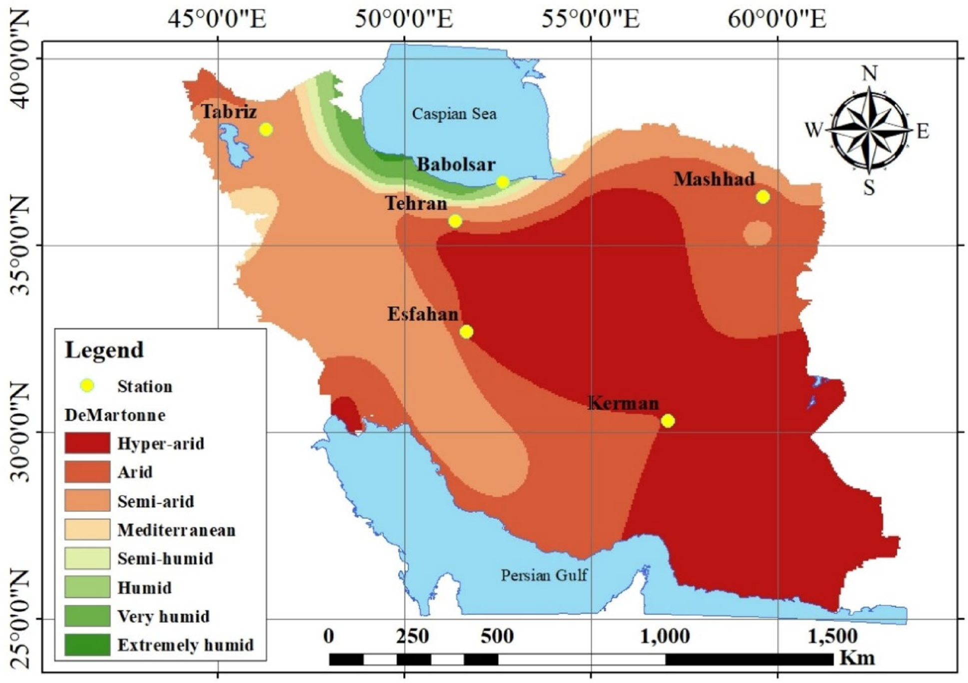

Fig. 1. Location of the weather stations in diverse climates based on the de Martonne climate classification (drawn by Arc Map 10.6.1 software).

Name	Lat.	Long.	Elev. (m)	AT_{max} (°C)	AT_{min} (°C)	APT (mm)	API (mm/day)	Climate (de Martonne)
Babolsar	36° 42′ N	52° 39′ E	−21	34.9	−1.0	894.5	12.2	Humid
Esfahan	32° 39N	51° 39′ E	1550	40.2	−9.1	121.0	5.2	Hyper Arid
Kerman	30° 17′ N	57° 05′ E	982	39.7	−13.3	135.5	5.3	Hyper Arid
Mashhad	36° 17′ N	59° 36′ E	1478	40.0	−14.3	246.9	6.1	Arid
Tabriz	38° 04′ N	46° 17′ E	1361	38.7	−14.7	283.0	5.3	Semi-Arid
Tehran	35° 43′ N	51° 20′ E	1191	41.1	−6.9	234.8	5.8	Arid

Table 1. The geographical information, long-term (1960–2021) mean of the ECIs, and climatic classification of the studied weather stations.

No	Index name	Symbol	Definition	Unit
1	Annual maximum of maximum temperature	AT_{max}	The annual maxima of daily maximum temperature	°C
2	Annual minimum of minimum temperature	AT_{min}	The annual minima of daily minimum temperature	°C
3	Total annual precipitation	APT	The annual sum of daily precipitation more than one millimeter	mm
4	Annual precipitation intensity	API	The ratio of annual precipitation to the number of wet days with precipitation more than one millimeter	mm/day

Table 2. Description of extreme climate indices considered in this study.

Cartesian coordinate system where the first and second half are placed on the horizontal (x) and vertical (y) axes, respectively. If the scatter points lie along the 1:1 (45°) line, no significant trend in the time series is concluded. However, if the points fall above or below the 1:1 line, the associated time series has an increasing or decreasing trend, respectively[28,32].

Power of trend in ITA method

To evaluate the significance of the trends in the ITA test, Şen[46] introduced an *S* statistic as the slope value of the trend and provided a *CL* for it as follows:

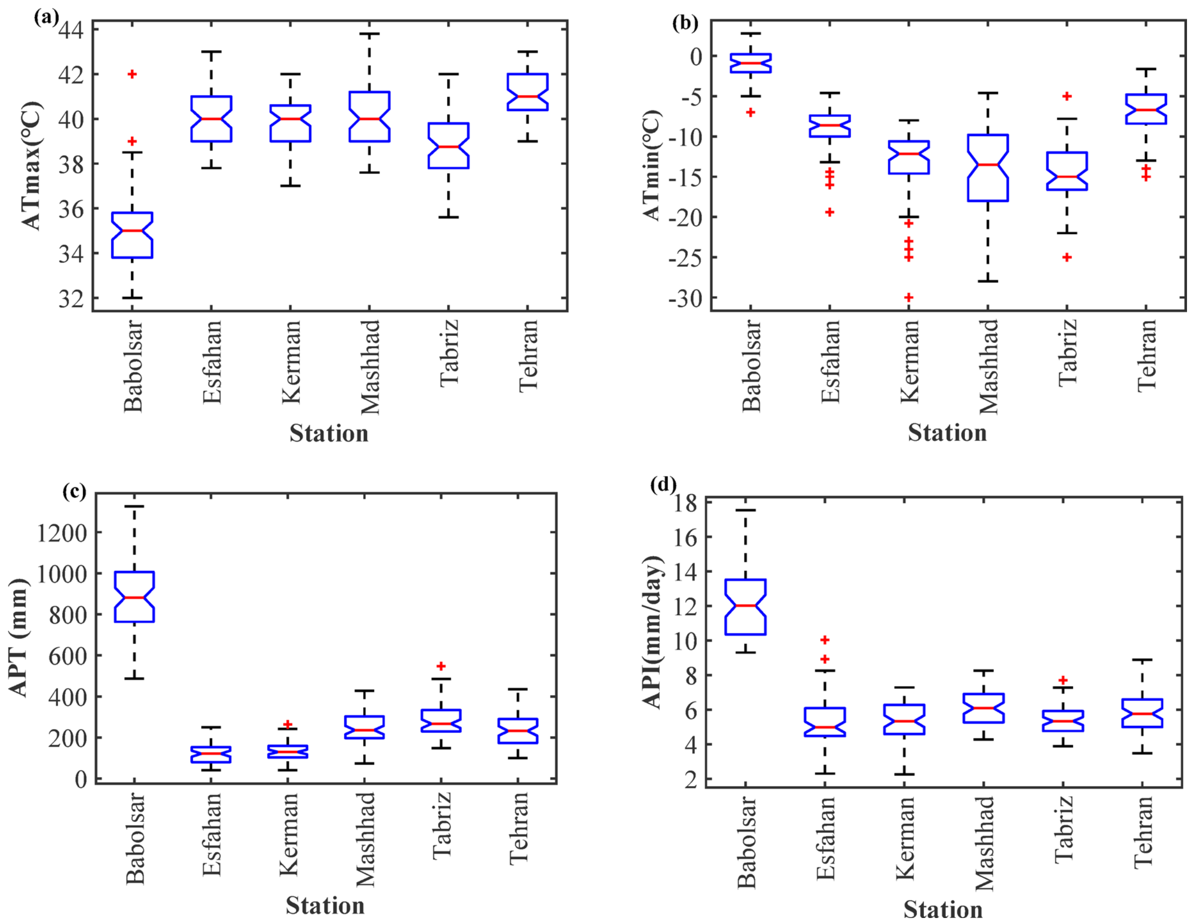

Fig. 2. Box plots of the (**a**) AT_{max}, (**b**) AT_{min}, (**c**) APT and (d) API in the studied stations. The boxes illustrate the 25th, 50th and 75th percentiles. The end points of the whiskers show the lowest (highest) datum within 1.5 times the interquartile range of the lower (upper) quartile.

$$S = \frac{2\left(\bar{y} - \bar{x}\right)}{N} \tag{1}$$

$$CL_{1-\alpha} = 0 \pm s_{cri}\sigma_s \quad , \quad \sigma_s = \frac{2\sqrt{2}}{N\sqrt{N}}\sigma\sqrt{1-\rho_{y,x}} \tag{2}$$

where, $\bar{x}$ and $\bar{y}$ are the average of the first and second sub-series, respectively, s_{cri} is the critical value of the Gaussian distribution function for the α percent significance level (SL), N is number of all data, σ is the standard deviation of all data, and $\rho_{y,x}$ is the correlation coefficient of the ascendingly sorted data of the first and second sub-series.

To quantify the value of the trend detected by the ITA test, Wu and Qian[40] proposed an indicator (D) as follows and claimed that it is on the same scale as the Z value of the M-K test:

$$D = \frac{1}{n}\sum_{i=1}^{n}\frac{10\left(y_i - x_i\right)}{\bar{x}} \tag{3}$$

where, n is number of points in the ITA graph, x_i and y_i are the value of the first and second sub-series, respectively for i^{th} point, and $\bar{x}$ is the average of the first sub-series.

Fuzzy-logic innovative trend analysis (FITA)

To enhance the capabilities of the ITA method for simultaneous trend analysis of ECIs at multiple levels, we proposed an innovative approach, called FITA, which integrates a set of fuzzy rules with the ITA diagram. Fuzzy rules imposed on a variety of hydrological analysis have been satisfactorily used in many studies[49–53]; however, to the best of the authors' knowledge, no study has explored their efficiency in conjunction with trend analysis of the extreme indices yet.

FITA plot

The FITA is a graphical trend analysing method (Fig. 3) that commences with determining the desired number of levels (N_l) and the associated fuzzy linguistic terms (N_f) exclusively based on expert opinion. Since no sharp distinctions usually exist between levels of ECIs, the number of fuzzy terms is suggested regarding the logic of the ITA method (Eq. 4).

$$N_f = N_l + 3 \quad , \quad N_l = 2,\ 3,\ 4, \ldots \tag{4}$$

Based on the selected N_p a threshold constant (TC) is defined to determine the bound of clusters. Like identifying N_p it should be noted that TC is determined based on expert opinion. Thus, the associated length of the clusters could be equal or unequal. In this study equal length is considered (Eq. 5).

$$TC = \frac{I_{max} - I_{min}}{N_l} \tag{5}$$

where the numerator $I_{max} - I_{min}$ represents the range of entire climate index *I*.

For a three-level (i.e., low, medium, and high) trend analysis with FITA (Fig. 3), the points of the FITA diagram (I_x, I_y) falls into one of six clusters, labelled as *low*, *medium*, *high*, *incremental transition*, *decremental transition*, *and outlier* according to the following fuzzy rules.

- If $I_{min}< I_x< I_{min}+ TC$ & $I_{min}< I_y< I_{min}+ TC$, then (I_x, I_y) *is low.*
- If $I_{min} + TC< I_x< I_{min}+2\ TC$ & $I_{min}+ TC < I_y< I_{min}+2\ TC$, then (I_x, I_y) *is medium.*
- If $I_{min} + 2TC< I_x< I_{max}$ & $I_{min} + 2TC< I_y< I_{max}$, then (I_x, I_y) *is high.*
- If $I_{min}< I_x< I_{min}+ TC$ & $I_{min}+ TC < I_y< I_{min}+2\ TC$, then (I_x, I_y) *is incremental transition.*
- If $I_{min}+ TC < I_x< I_{min}+2\ TC$ & $I_{min}+2\ TC < I_y< I_{max}$, then (I_x, I_y) *is incremental transition.*
- If $I_{min} + TC< I_x< I_{min}+2\ TC$ & $I_{min}< I_y< I_{min}+ TC$, then (I_x, I_y) *is decremental transition.*
- If $I_{min} + 2TC< I_x< I_{max}$ & $I_{min} + TC< I_y< I_{min}+2\ TC$, then (I_x, I_y) *is decremental transition.*
- If $I_{min}< I_x< I_{min}+ TC$ & $I_{min}+2\ TC < I_y< I_{max}$, then (I_x, I_y) *is outlier.*
- If $I_{min} + 2TC< I_x< I_{max}$ & $I_{min}< I_y< I_{min}+ TC$, then (I_x, I_y) *is outlier.*

here, *TC* denotes one-third of the range of the entire samples.

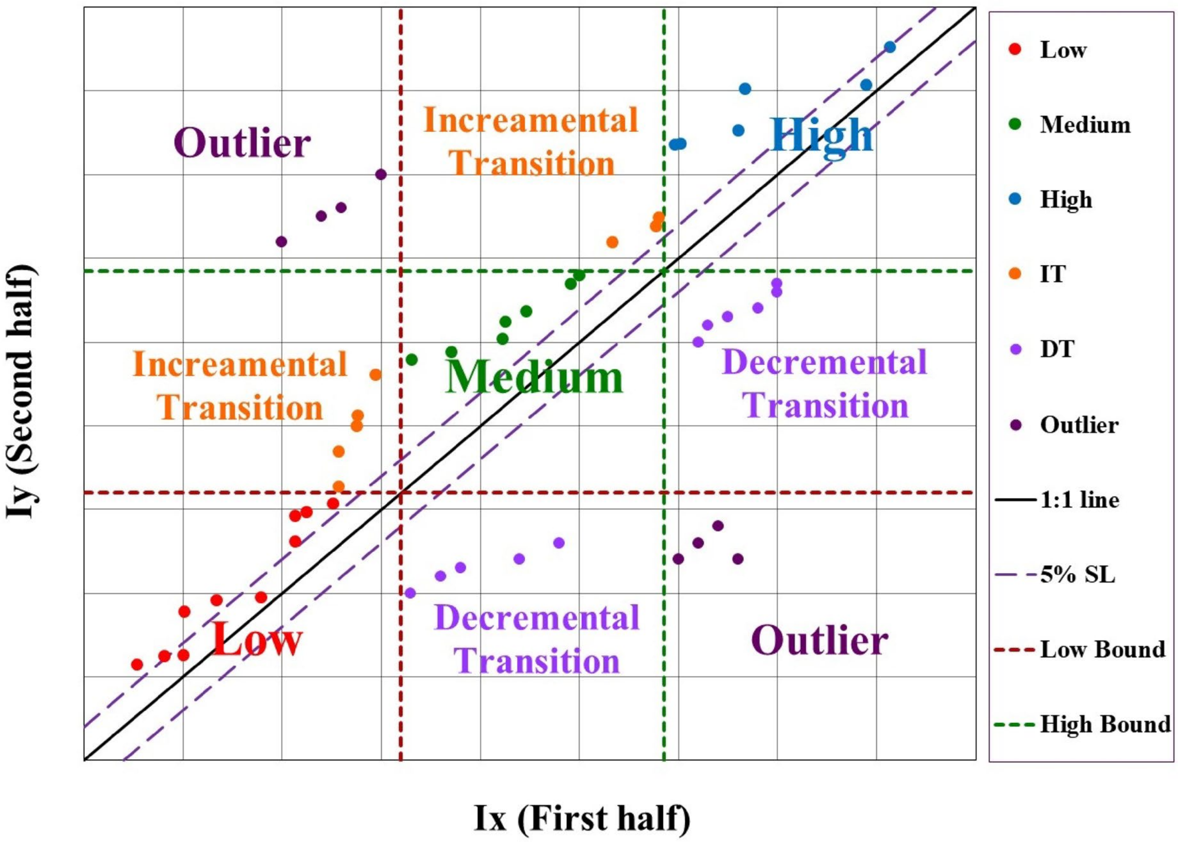

Fig. 3. The schematic of FITA diagram evolved for three-level (low, medium, high) trend analysis of extreme climate indices.

The incremental transition clusters are the zones where I_y is one level more than I_x, i.e., for three levels, I_x is at the level of low (medium), while I_y is at the level of medium (high). In contrast, in the points belonging to the decremental transition cluster, I_y is one level less than I_x, i.e., I_x is at the level of medium (high), while I_y is at the level of low (medium). The points that fall into the outlier cluster have more than one level difference between the level of I_x and I_y, i.e., for three levels, I_x is at the level of low (high) while I_y is at the level of high (low). Since in the ITA plot, the data in each of the first and second half have been sorted in ascending order, if there is/are a point/points in the outlier clusters, it means that there is an abnormal condition like a jump in the data; so that, if the vertical outlier cluster where I_x is in low and I_y is in high level contains data, then the I_y of other data is also in the high level, which means that there is an increasing jump in the second half compared to the first half. Conversely, if the horizontal outlier cluster where I_x is in high and I_y is in low level contains data, the I_y of other data is also necessarily in the low level, which means that there is an decreasing jump in the second half compared to the first half.

Like the classic ITA, positive, negative, or insignificant trend conditions in the low, medium, and high levels (classes) are determined concerning the distribution of the points. If they scattered above (below) 5.0% SL, a positive (negative) trend must be designated at the confidence level (*CL*) of 95% for the associated level. A uniform distribution of the points within 5.0% SL boundaries represents an insignificant trend at *CL* of 95%[34[,54]. Since the points in the incremental and decremental transition clusters reveal a considerable difference between the value of I_x and I_y, greater numbers of the points in these clusters indicate stronger increasing and decreasing trends, respectively for the level corresponding to the I_x. The points in the outlier cluster should not be taken into account during trend analysis as they may exhibit a jump event.

Power of trend in FITA method

To quantify the power of trend at each level (i.e., classified data) and entire time series, Grow Percent (*GP*) and Total Grow Percent (*TGP*) indices are defined based on the growth of the samples in the second half compared to the first half for each level in *GP*, and for all data in *TGP*.

$$GP_i = \frac{\sum_{j=1}^{n_i}(I_{yj} - I_{xj})}{n_i.(I_{max} - I_{min})} \times 100 \; ; \qquad (i = 1,\ 2,\ \ldots\ , N_l) \tag{6}$$

$$TGP = \frac{\sum_{j=1}^{N}(I_{yj} - I_{xj})}{N.(I_{max} - I_{min})} \times 100 \tag{7}$$

where n_i is the count of scatter points in which I_x lies at the level *i*, ($I_{yj} - I_{xj}$) indicates the distance of j^{th} scatter point from 1:1 line, when I_x is in the level *i*, *N* is the number of all points, and $(I_{max} - I_{min})$ is the range of data.

The values of *GP* and *TGP* fall within the range of *–Inf.* to *Inf.* The positive and negative values imply increasing and decreasing trends, respectively. The absolute values between 0 and 5 reveals *no significant trend* in the data. The absolute values of *GP* and *TGP* between 5 and 10 reveals a 5–10% deviation of the data from the bidirectional line, considered as a *slightly significant trend*, and the absolute values greater than 10, exhibits a considerable deviation of data, suggest a *significant trend* in the data.

Mann–Kendall (M–K) trend test

The M-K test is a nonparametric trend test, presented by Mann[55] and completed by Kendall[56]. The advantage of this method compared to other trend tests is that it is based on the ranking of the data, and the value of data does not affect the results of the test; so, this test is applicable for skewed data, and the data does not require to be normally distributed[57]. In the M-K test, the null hypothesis (H_0) which is the independence and randomness of the data (Absence of trend) is evaluated against the alternative hypothesis (H_1) which is the presence of a trend in the data. Suppose $x_1, x_2, \ldots, x_n$ is a data series, then the *S*-statistic is obtained as follows:

$$S = \sum_{k=1}^{n-1} \sum_{j=k+1}^{n} sgn(x_j - x_k) \tag{8}$$

$$sgn\,(x_j - x_k) = \begin{cases} +1 & if \quad (x_j - x_k) > 0 \\ 0 & if \quad (x_j - x_k) = 0 \\ -1 & if \quad (x_j - x_k) < 0 \end{cases} \tag{9}$$

Regarding the use of *Sgn* function for calculation of *S*, the rank of data could be applied rather than their values. The statistic of M-K test (*Z*) which has normal distribution function is as Eq. 10.

$$Z = \begin{cases} \frac{S-1}{\sqrt{Var(S)}} & if \quad S > 0 \\ 0 & if \quad S = 0 \\ \frac{S+1}{\sqrt{Var(S)}} & if \quad S < 0 \end{cases} \tag{10}$$

$$Var\,(S) = \frac{n\,(n-1)\,(2n+5) - \sum_{i=1}^{m} t_i(t_i - 1)(2t_i + 5)}{18} \tag{11}$$

where *n* is the number of data, *m* is the number of tied groups each of which contains repeated data, and t_i is the number of repeated data in the i^{th} group.

The M-K test is a two-tailed test; so, H_0 is accepted at the CL of $(1-\alpha)\%$ if $|Z| \leq Z_{\alpha/2}$. Otherwise, the H_1 is accepted which means that the data series has significant trend. When the data exhibit trend, the positive and negative values of the *S*-statistic indicate increasing and decreasing trend, respectively. in this study, the significance of the trends is evaluated at *CL* of 95% ($|Z| \leq 1.96$).

Sen's slope (SS)

The SS[58] is a non-parametric method to estimate the magnitude of slope for an existing linear trend. The *SS* value for a data series $x_1, x_2, \ldots, x_n$ is obtained as follows:

$$SS = Median\left(S_k\right), \quad k = 1, \ldots n\left(n-1\right)/2 \tag{12}$$

$$S_k = \frac{x_i - x_j}{i - j}, \quad i = 1, \ldots, \; n-1, \quad j = i+1, \ldots, n \tag{13}$$

where, S_k is the slope between k^{th} pair of data. For *n* data, the number of unrepeated pair data is *n(n-1)/2*.

Results

Trends in annual maximum of the maximum temperature (AT_{max})

The results attained by three-level FITA applied on AT_{max} were demonstrated in Fig. 4. It is observed that different numbers of points are located within the clusters, which implies a non-uniform distribution of data during the first and second half. In Babolsar station, there were many points in the low and incremental transition clusters with low AT_{max} in the first half mostly placed above the 5% SL line. Therefore, we can conclude that a significant increasing trend exists at the low values of AT_{max} (i.e., local minima are increasing). Although there were fewer points in the medium and high classes of this station, a significant decreasing trend was inferred at the high level (i.e., local maxima are decreasing). In Esfahan, Kerman, and Mashhad stations, there were lots of points in the incremental transition clusters with low and medium AT_{max} in the first period, which exhibited a considerable increasing trend in the low and medium levels; but instead, there was no point at the high levels of Esfahan and Mashhad. Concerning the number of points in the incremental transition cluster of the medium level and no points at the high cluster in both stations, it can be concluded that a considerable increase occurred in high values of AT_{max} during the second period (1991–2021) compared to the first one (1960–1990). Figure 4 also shows a significant increasing trend at the high level of Kerman station. Besides, there were no considerable trends at the low and high levels of AT_{max} in Tehran and Tabriz; however, a slightly increasing trend was recognized at the medium level of both stations.

The power of the three-level trend analysis of AT_{max} using the FITA method was tabulated in Table 3. The *TC* values vary between 1.33 (Tehran) to 3.33 (Babolsar). The value of *TC* was similar for Kerman and Esfahan with the same climates; however, it was different for Mashhad and Tehran which have arid climates. The power of trends detected by FITA at each level by the *GP* index (Table 3) also confirmed a remarkable increasing trend ($GP > 20$) in the low and medium levels of Esfahan, Kerman, and Mashhad, as well as the high level of Kerman.

Also, a slightly significant increasing trend ($5 < GP < 10$) was revealed at the low levels of Babolsar and Tehran, and the medium levels of Tabriz and Tehran, while a significant decreasing trend ($GP = 17$) was observed at the high level of Babolsar. At the other levels, there was no significant trend ($GP < 5$) at Babolsar, Tabriz, and Tehran stations.

Assessment of the *TGP* values compared to the *GP* values (Table 3) revealed that the value of the *TGP* at Babolsar, Esfahan, and Mashhad stations, where there was a substantial difference between the *GP* values, cannot reflect the trend at each level. For example, a considerable decreasing trend at the high level ($GP = -17.00$), an increasing trend at the low level ($GP = 9.417$), and insignificant trend at the medium level ($GP = -0.500$) are seen considering AT_{max} at the SL of 5% at Babolsar station. However, the value of *TGP* indicates a slightly increasing trend ($TGP = 5.581$) in this ECI based on all data. Although there was no trend at the high levels of Esfahan and Mashhad, the *TGP* revealed a remarkable increasing trend of AT_{max} ($TGP > 23$) at both stations due to the existing trend in their two other levels.

Trends in annual minimum of the minimum temperature (AT_{min})

The trend analysis of AT_{min} by the FITA method (Fig. 5) exhibited a remarkable increasing trend at all three levels of Babolsar and Mashhad, at the low and medium levels of Kerman and Tehran, as well as at the low level of Tabriz. The considerable number of points in the incremental transition clusters in these stations indicated a strong increasing trend in the low and medium values of the AT_{min} at the SL of 5%.

Figure 5 also shows no significant trend in any levels of AT_{min} in Esfahan at the SL of 5%. A similar condition was almost observed for the high level of Kerman, and Tabriz. However, there was a slightly increasing trend in the medium values of the AT_{min} in Tabriz, as well as in the high values of Tehran.

Evaluation of the *TC* values (Table 4) illustrated its range between 3.27 (Babolsar) to 7.80 (Mashhad). Like AT_{max}, the value of *TC* was not similar neither for Kerman and Esfahan, nor for Mashhad and Tehran which have the same climates; as a result, the range of clusters was not equal for these stations. The power of trend in each of levels of the AT_{min} index revealed that there was a considerable increasing trend ($GP >= 20$) in all three levels of Mashhad, and in the low level of all other stations other than Esfahan.

Also, a significant increasing trend ($GP > 10$) was demonstrated in the medium and high levels of Babolsar, as well as in the medium level of Kerman, and Tehran. A slightly significant increasing trend ($5 < GP < 10$) was observed at the medium level of Tabriz and at the high level of Kerman and Tehran. Although the FITA graph showed no trend for Esfahan, a slightly decreasing trend was revealed for all levels of this station which was significant at the SL of 5% only for the low level.

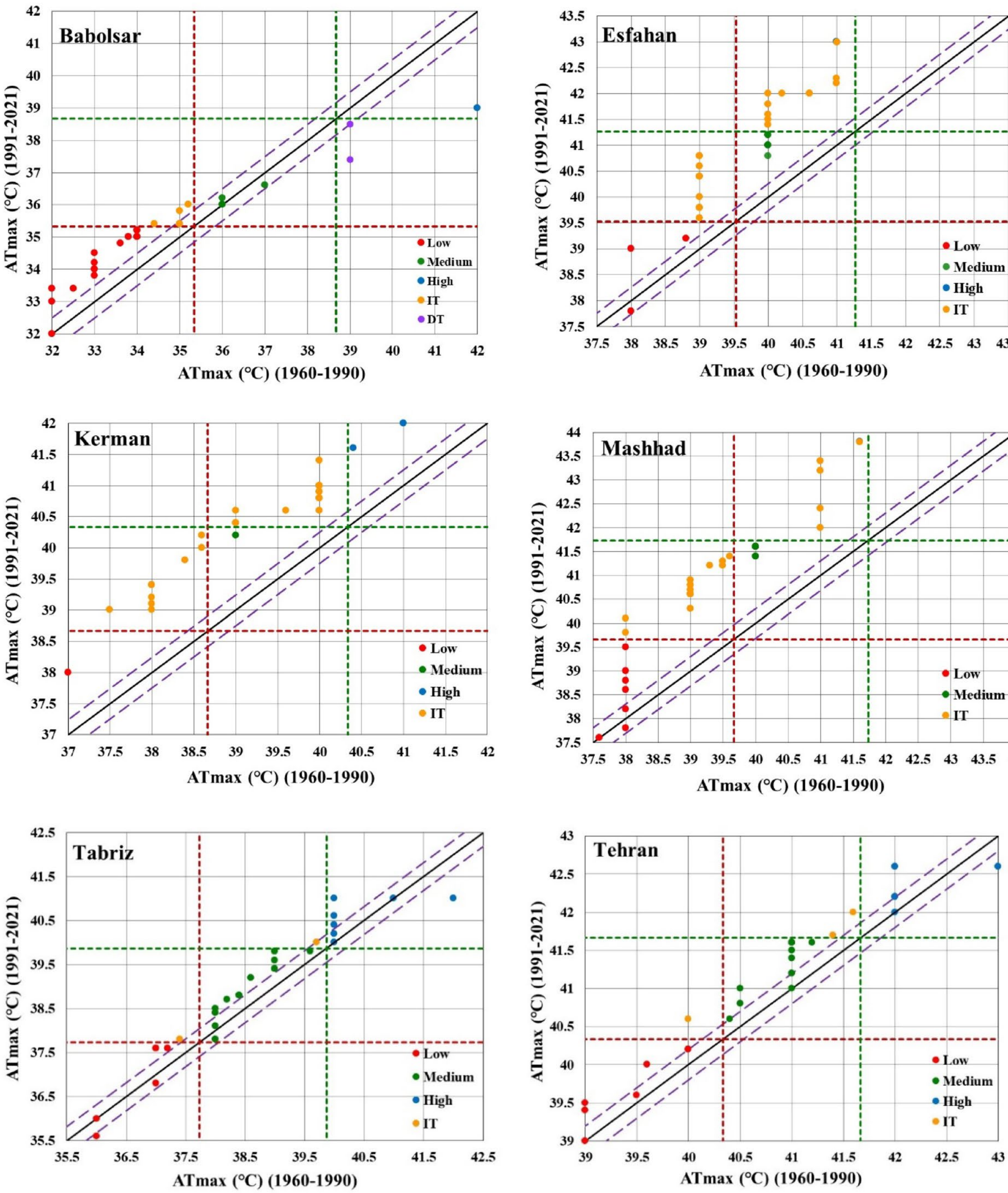

Fig. 4. The graphs of FITA method for AT_{max} indicator.

The value of the *TGP* index indicated a significant increasing trend (*TGP* > 10) at all stations except Esfahan. However, the value of this index could not illustrate the trend at each level, when a significant difference was observed between the *GP* values; this condition was visible especially at Esfahan, Kerman, Tabriz, and Tehran stations.

Trends in total annual precipitation (APT)

The trend analysis of the APT index by the FITA method (Fig. 6) revealed diverse conditions in the studied stations; in Babolsar, an increasing trend was detected in the high level, while a slightly increasing and decreasing trend was observed in the medium and low levels, respectively. While an increasing trend was inferred in all levels of APT for Esfahan, the medium and high levels of APT in Tabriz had a significant decreasing trend with several points in the decremental transition clusters. However, no significant trend in any levels of the APT in Kerman, Mashhad, and Tehran stations was detected.

Station	Range		TC	Grow percent (GP)			Total grow percent (TGP)
	I_{max}	I_{min}		low	Medium	High	
Babolsar	42.00	32.00	3.33	**9.42**	−0.50	**−17.00**	**5.58**
Esfahan	43.00	37.80	1.73	**20.05**	**26.70**	0.00	**23.70**
Kerman	42.00	37.00	1.67	**26.18**	**21.33**	**22.00**	**23.10**
Mashhad	43.80	37.60	2.07	**21.37**	**26.98**	0.00	**23.36**
Tabriz	42.00	35.60	2.13	3.13	**5.88**	2.68	4.54
Tehran	43.00	39.00	1.33	**7.50**	**9.67**	3.13	**7.42**

Table 3. Power of multi-level trend analysis in AT_{max} index detected by FITA method for each level and all data. *Bold values are significant trends at the confidence level of 95%.

Unlike the AT_{max} and AT_{min} indices, the value of *TC* (Table 5) for the APT index was similar for the stations with the same climates while its maximum value belonged to Babolsar station (*TC* = 279.86 mm) with a humid climate, and its minimum one (*TC* = 74.14 mm) was for Kerman station with hyper-arid climate. Assessing the power of trend in each of the levels of the APT index also confirmed that there were significant increasing trends ($GP >= 10$) in all levels of Esfahan, and the high level of Babolsar, while the decreasing ones were observed in the medium and high level of Tabriz. Although no trends were detected by the FITA graph for Kerman, Mashhad, and Tehran, a slightly significant trend at the SL of 5% ($5 < GP < 10$) was indicated for low and medium levels of Kerman, the low level of Mashhad, and the medium level of Tehran. All other levels of these stations as well as the low and medium levels of Babolsar had not any significant trend in APT at the SL of 5%.

Evaluation of the *TGP* values (Table 5) revealed a significant increasing and decreasing trend ($TGP > 10$) for Esfahan and Tabriz, respectively, and a slightly significant decreasing trend ($5 < TGP < 10$) for Kerman. However, any significant trend was not identified based on this index at Babolsar, Mashhad, and Tehran stations at SL of 5%. But there were significant trends at the high, low, and medium levels of these stations, respectively.

Trends in the annual precipitation intensity (API)

The trend analysis by the FITA method for the API index (Fig. 7) indicated a significant increasing trend at the low and medium levels of Babolsar and Esfahan stations, so that a large number of points were observed in the incremental transition clusters in both stations, and few and no number of points were placed in their high clusters. Also, all levels of API in Kerman and Mashhad had significant increasing trends at the SL of 5% which were more confident for the low level of Kerman and medium and high level of Mashhad. Although the low level of API in Tabriz had a significant increasing trend, any trend was not observed in the medium or high levels of this station. However, a slightly increasing trend was inferred for all levels of Tehran which was more significant for the high level.

Assessment of the API range and its *TC* values in the studied stations (Table 6) showed that the minimum and maximum range of API belonged to Tabriz and Babolsar, respectively. Unlike the APT index, the condition of stations in terms of *TC* values was independent of their climates.

The *GP* values for this index indicated significant increasing trends ($GP > 10$) for the low and medium levels of Babolsar and Esfahan, the low level of Kerman and Tabriz, as well as the medium and high levels of Mashhad. Also, a slightly increasing trend ($5 < GP < 10$) was proved for all levels of Tehran, the medium and high levels of Kerman and the low level of Mashhad. However, the value of the *TGP* index revealed significant increasing trends for all stations at 5% SL, while no trend was detected at the high levels of Babolsar and Esfahan, as well as at the medium and high levels of Tabriz.

FITA results vs. M-K, SS, and ITA

Table 7 compares the power of trends and their consistency attained by FITA, M-K, SS, and ITA. It was observed that in most cases with remarkably significant trends, the results of the *TGP* agree with the *Z* value of the M-K test in terms of reliability at the CL of 95%. However, the magnitude and even sign of their values are inconsistent in some cases. For example, FITA shows a more significant overall trend in AT_{min} at Tehran station ($TGP = 19.042$) in comparison to Babolsar ($TGP = 17.380$). However, the magnitude of their Z values of the M-K test was the opposite. An analogous situation was observed for AT_{max} at these stations. Based on *TGP*, the existing trends were significant (at the CL of 95%) at both stations while the trend at Tehran station was not identified as significant at the same CL by M-K test. A similar condition was recognized in the trend of APT at Esfahan and Kerman stations.

Besides, a decreasing trend was identified in all data of the AT_{min} index in Esfahan according to the FITA test, which was insignificant; however, the M-K test showed an increasing trend in this ECI, which was also insignificant. In several other cases such as the trend in APT at Esfahan as well as the trends in API at Kerman, Tabriz, and Tehran stations, the FITA identified significant trends at the SL of 5% while the M-K test implies insignificant trend at that CL.

According to Table 7, the *SS* variation agrees neither with *Z* nor *TGP* values in all the ECIs and stations. For example, the highest *SS* value for AT_{max} was calculated at Mashhad station ($SS = 0.037$, $Z = 3.460$, $TGP = 23.361$) while the greatest *Z* and *TGP* values were obtained at Kerman ($Z = 4.280$, $SS = 0.028$, $TGP = 23.097$) and Esfahan ($TGP = 23.697$, $Z = 3.920$, $SS = 0.028$) stations, respectively. Similar results were also observable in the other ECIs.

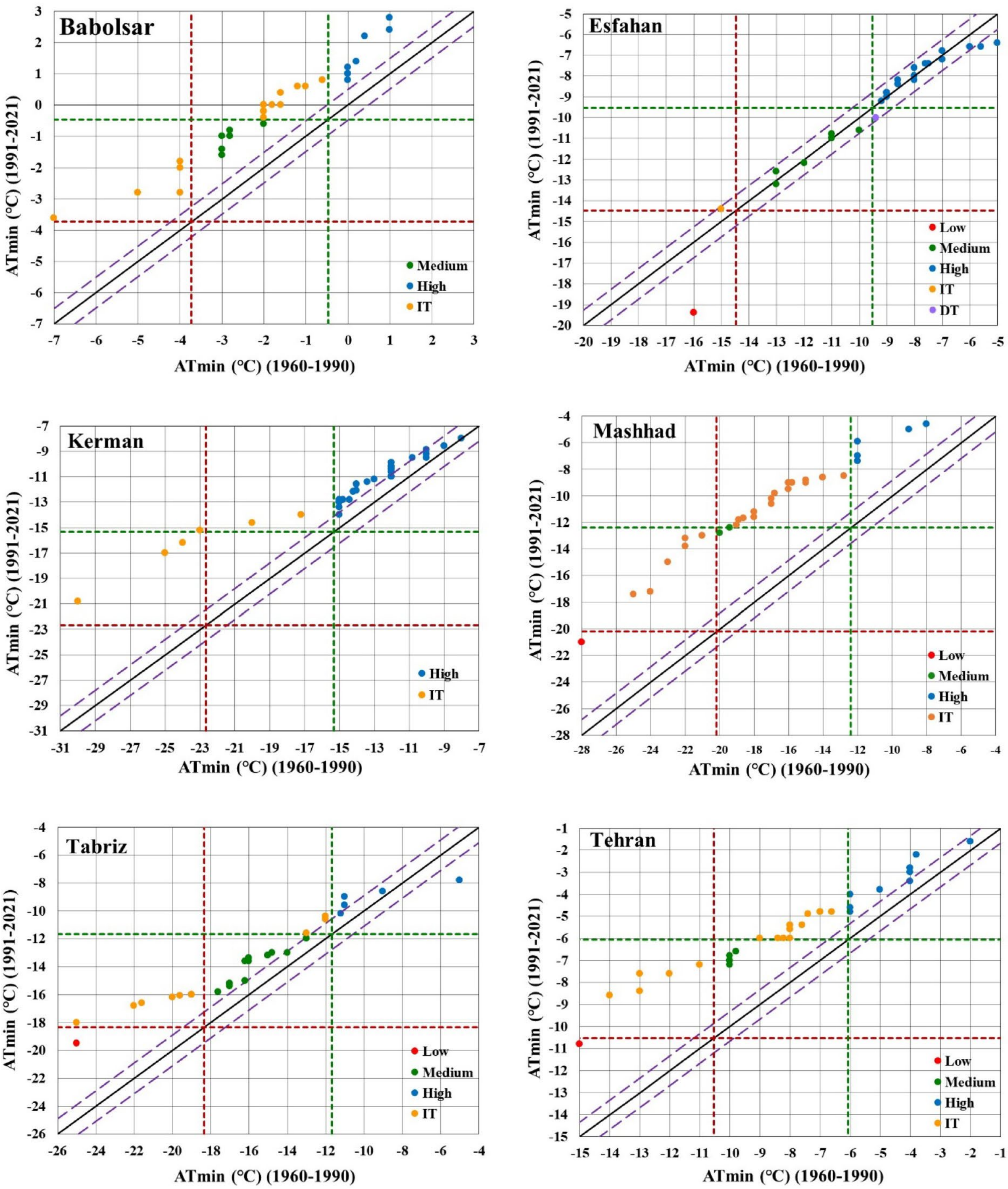

Fig. 5. The graphs of FITA method for AT_{min} indicator.

This means that the ranking of the stations in terms of trend intensity is somewhat different based on these three methods.

The power of trends detected by the ITA (i.e., *D* and *S* indices) was found inconsistent with the *Z* index as only in a few cases the absolute value of *D* was like *Z*. Moreover, directions of overall trends in AT_{min} determined by *D* disagree with those of *Z*, *SS*, and *TGP* at all stations. For instance, while *D* indicates a decreasing trend at all stations (except Esfahan), the other tests show a significant increasing trend. At Esfahan station, *D*, *Z*, and *SS* imply an increasing trend, while *TGP* and *S* revealed a decreasing trend. The Table also proves that the trend direction detected by *S* and *TGP* are consistent at all ECIs/stations; however, their significance were different at the CL of 95% in several cases, like AT_{max} of Tabriz, AT_{min} of Esfahan, and APT of Babolsar, Mashhad, and Tehran.

Station	Range		TC	Grow percent			Total grow percent (TGP)
	I_{max}	I_{min}		low	Medium	High	
Babolsar	2.80	−7.00	3.27	**22.45**	**17.91**	**13.01**	**17.38**
Esfahan	−4.60	−19.40	4.93	**−9.46**	−0.45	−0.56	−1.11
Kerman	−8.00	−30.00	7.33	**37.27**	**19.55**	**6.85**	**11.60**
Mashhad	−4.60	−28.00	7.80	**32.69**	**27.54**	**19.74**	**27.61**
Tabriz	−5.00	−25.00	6.67	**22.50**	**8.67**	2.00	**11.16**
Tehran	−1.60	−15.00	4.47	**34.58**	**18.98**	**8.79**	**19.04**

Table 4. Power of multi-level trend analysis in AT_{min} index detected by FITA method for each level and all data. [*]Bold values are significant trends at the confidence level of 95%.

Discussion

As previously described, the FITA approach enhances the conventional ITA method and facilitates multi-level trend analysis via clustering ECIs based on fuzzy logic rules. The points' frequency at each cluster as well as their distance from the bidirectional line are used to interpret the potential trend at each level. The higher frequency of the samples in the incremental and decremental transition clusters reveals important changes in the data and exhibits significant trends in the level corresponding to the transitional cluster.

The N_l for trend analysis using FITA is recommended to be chosen according to the (i) number of data, (ii) their range, and (iii) type of ECI so that at least one of the clusters belonging to each level (e.g., the clusters of low and its incremental and decremental transitions for the level of low) contains data. For long-term historical data with a wide range of variation, a greater N_l could be chosen if it is scientifically meaningful. The value of the extreme climate indices is usually assessed in three or five levels[38,40,41,59,60]. Regarding the length, range, and type of al ECIs, a total of three levels were suggested and utilized in this study.

Also, the length of levels (*TC*) can be defined unequally, depending on the range of the given climatic index, its defined levels (if exists), as well as the expert opinion. The levels' boundaries may be defined concerning the interquartile range (IQR) of the observed data. In this condition, the *TC* of the levels will be unequal; however, each level will necessarily contain the same number of observations. The quartile-based segmentation could destroy the hydrologic concepts of low, moderate, and high values, as considered in the present study. By contrast, the level selection according to a hydrological/meteorological perspective, particularly for ECIs (as done in this study), facilitates the interpretability of trend in each level corresponding to the real conditions, while there is an unequal frequency of samples at each level. For example, there was only one sample point in the high level of AT_{max} at Babolsar station which reveals a trend in the extreme high values of AT_{max} in the second period compared to the first one (each point in the FITA graph corresponds to two values in the first and second period). The value of the *GP*, in this case, indicated that the maximum value of AT_{max} in the second period has decreased by 17% of all data ranges as compared to the first period. Therefore, it is concluded that the level/cluster resolution is better determined via a trade-off between the N_l and frequency of samples at each cluster. If there is no data in the clusters related to a level, it means that either N_l should be decreased, or the boundary of clusters may be changed.

Since FITA is a graphical method, an external measure is required to quantify the magnitude of the trend. In this study, *GP* and *TGP* measures were proposed and compared to some existing indices including *D*, *S* (presented for ITA test), as well as *SS*, and *Z*. The attained *TGP* values (for all data) revealed its excellence compared to its counterparts. The superiority of *GP* and *TGP* over *D* is in two aspects; First, *D* is applicable for the variables having zero or positive values like precipitation. As shown in Table 7, this index may show a reverse trend for the variables with negative values such as AT_{min}. By contrast, both *GP* and *TGP* can be used for both positive and non-positive values. Secondly, Wu and Qian[40] presented the *D* index as a comparable indicator with the *Z*-statistic of the M-K test; however, our results at all stations (Table 7), confirmed the results of Gumus, et al.[34]and Cui, et al.[45] who reported that the values of this index are much far from the *Z*-statistic when they are applied for streamflow, precipitation and temperature. Hence, the trend significance cannot be interpreted compared to similar the *Z*-statistic in each *CL*. In addition, evaluation of the slope values of the ITA test (*S* index) and its *CL* (Table 7) indicated that based on the *CL* value, all of the slopes were detected as significant because the correlation coefficient (ρ) in the *CL* formula is calculated for the ascendingly sorted data of the first and second sub-series. This problem in quantifying trend significance using *S* needs additional attention of its users. However, *GP* and *TGP* values exhibit the magnitude of the trend for the classified and entire data, respectively, while they can be interpreted at different confidence levels based on their values. Therefore, they are suggested to be used as robust alternatives for *D* and *S* when using the ITA and FITA tests.

The results of this study revealed that the overall trends detected using the FITA agree with those of the M-K and SS tests, specifically in the cases showing considerable significant trends. This finding is also consistent with the results of Gumus, et al.[34], Nourani, et al.[59], and Kişi, et al.[33]. However, no relation existed between the *Z*-statistic, SS, and *TGP* values. Our results also showed that the slope values of the SS test did not have any relation with those of the ITA test (*S* index). Therefore, the magnitudes of the trends detected by these methods were different in several cases, which confirmed the results of Danandeh Mehr, et al.[38] and Kişi, et al.[33] regarding the results of the M-K and SS tests. Moreover, the FITA revealed a negative trend in AT_{min} at Esfahan station while the M-K and SS tests revealed a positive trend at the SL of 80% for it. Other indices of the ITA (*S* and *D*) also indicated a decreasing trend in this case (*D* index shows a reverse trend for AT_{min}). Figure 8 reveals why a

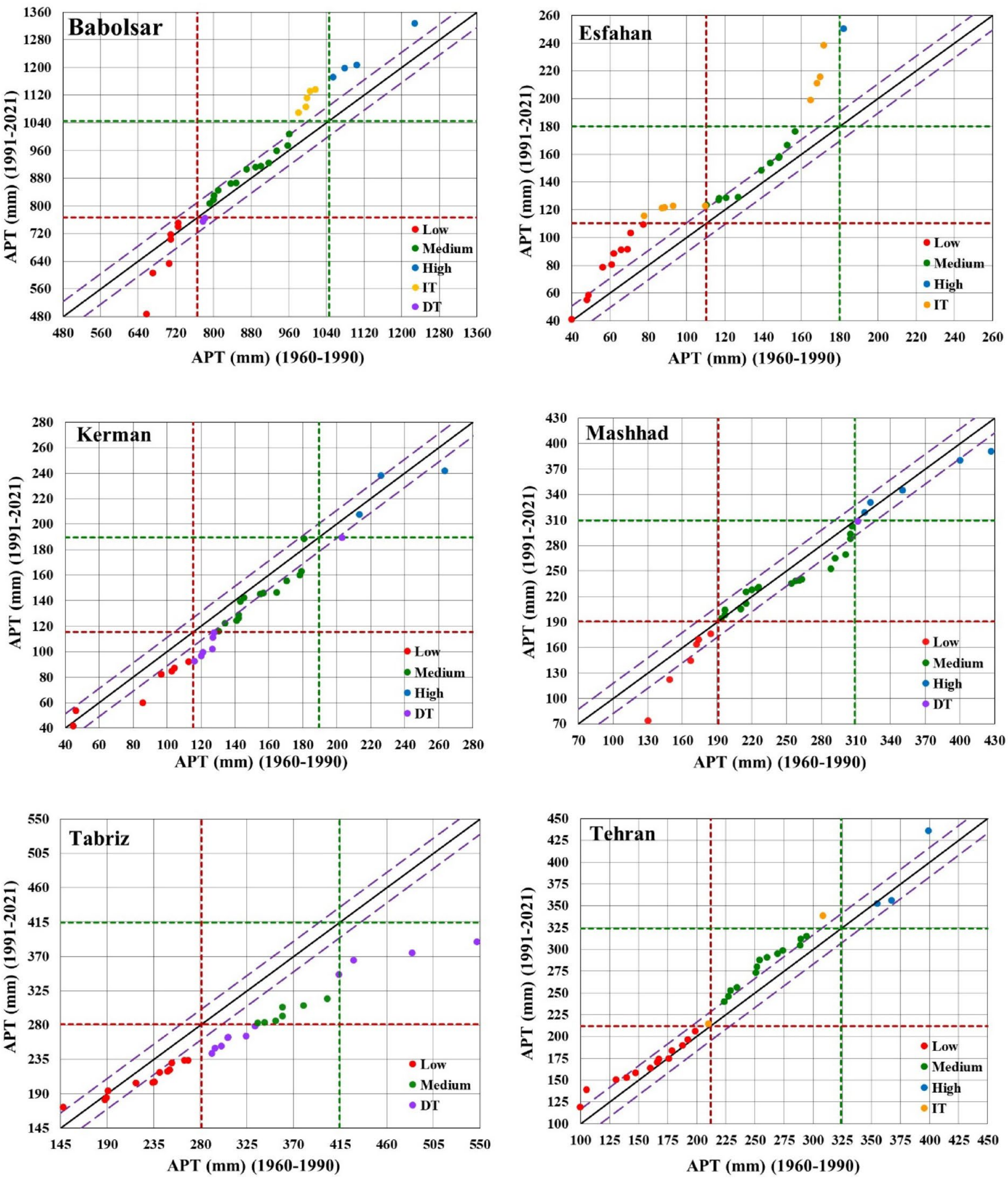

Fig. 6. The graphs of FITA method for APT indicator.

negative trend detected for AT_{min} in Esfahan by the FITA while a positive one was detected by the M-K test. In this figure, a linear regression was applied to the entire data (Fig. 8a) and compared to another linear regression that was applied to the scatter plot of the second-half vs. first-half of data without any sorting (Fig. 8b). The positive slope of the linear regression of the entire data (Fig. 8a) shows a slightly increasing trend in all data of AT_{min} detected by the M-K test. But, the negative slope of the linear regression in Fig. 8 (b) reveals that the AT_{min} values in the second half are smaller than the first half, which confirms the decrease trend detected by the FITA for AT_{min}. Indeed, it is concluded that the methodology of trend detection in these tests led to different results, which confirmed the results of Chervenkov and Slavov[31]Amirataee and Zeinalzadeh[61] and Rehman[29]. However, it seems that according to the data, the trends detected by the FITA and ITA methods are more reliable. A comparative analysis between the *GP* and *TGP* values revealed that the trend detected at multiple level may differ from the overall trend in terms of both sign and power. This finding was in line with those of Kisi and Ay[62],

Station	Range		TC	Grow percent			Total grow percent (TGP)
	I_{max}	I_{min}		low	Medium	High	
Babolsar	1325.80	486.21	279.86	−4.77	4.53	**12.81**	3.50
Esfahan	250.04	40.28	69.92	**10.78**	**9.49**	**32.26**	**10.85**
Kerman	263.67	41.25	74.14	**−6.20**	**−6.61**	−3.44	**−6.11**
Mashhad	427.23	73.13	118.03	**−6.28**	−2.99	−2.85	−3.60
Tabriz	547.61	148.01	133.20	**−4.60**	**−14.65**	**−25.18**	**−11.79**
Tehran	435.64	100.38	111.75	2.58	**6.87**	2.03	4.46

Table 5. Power of multi-level trend analysis in APT index detected by FITA method for each level and all data. *Bold values are significant trends at the confidence level of 95%.

Dabanlı, et al.[63], Caloiero, et al.[36] and Danandeh Mehr, et al.[38] that reported the greater power of the ITA test for detecting the correct trends in the classified data.

Our results indicated considerable differences in the ranges of AT_{max} and AT_{min} at the stations located in the same climate. However, the range of precipitation based ECIs was similar in those stations. Therefore, a similar *TC* value cannot be considered for temperature classification at the stations even with similar climates. Also, we found that the increasing trend in the AT_{min} is more significant than the increasing trend detected in AT_{max} in almost all the stations. This result agrees with the results of Kamali, et al.[25], Chaparinia, et al.[24], Alavinia and Zarei[19], Rahimi, et al.[18] and Soltani, et al.[22] attained by the M-K and SS tests. The results also showed that the highest increase occurred in the low level of both indices, which was not assessed in the previous studies. Moreover, our results exhibited an increasing trend in the API index at the SL of 5% in all stations, which agrees with the results of Alavinia and Zarei[19]Rahimi, et al.[18] and Rahimzadeh, et al.[26]. However, different increasing and decreasing trends were detected in the APT, which were not significant in half of the stations. These outcomes were also consistent with those of Chaparinia, et al.[24], Alavinia and Zarei[19], Fathian, et al.[23], Ghiami-Shamami, et al.[21] and Soltani, et al.[22].

Conclusions

In this study, a new approach, named FITA, based on incorporating the fuzzy logic rules with the graphical ITA was presented to facilitate multi-level trend analysis of ECIs. To quantify the trends detected by the FITA method at each level and whole data, two new statistics (i.e., GP and TGP) were proposed, respectively. The advantages of the new indices were explained over two indices, *D* and *S* (*CL*), previously presented for ITA test. The method was applied for four ECIs derived for six stations located in different climates across Iran, and the results were compared to those of the M-K and SS tests. Overall, we found that the trends identified by the FITA are consistent with those attained by the M-K and SS tests at the confidence level of 95% when significant overall trend exists in ECIs. However, the trend power calculated by the *TGP* is not consistent with those of the *Z*-statistic or slope of the SS test. The FITA can capture trends in more detail and provide more insights in temporal variation of ECIs.

The results also showed significant positive trends in the AT_{max}, AT_{min}, and API indices, particularly pronounced at the lower levels of these indices across almost all stations. However, diverse trends—both increasing and decreasing—were observed in the APT index, with some trends being statistically significant at the confidence level of 95% in certain stations. The synchronized increase in AT_{max}, AT_{min}, and API suggests that drier lands could be more prone to flash flood events. Although FITA was applied for ECIs and demonstrated through three-level trend analysis in the case studies, it has the potential to be applied to other climate variables at multiple levels, especially those that have a classification for their data range like drought indices. Future research can focus on exploring the strengths and limitations of FITA for application to various climate variables.

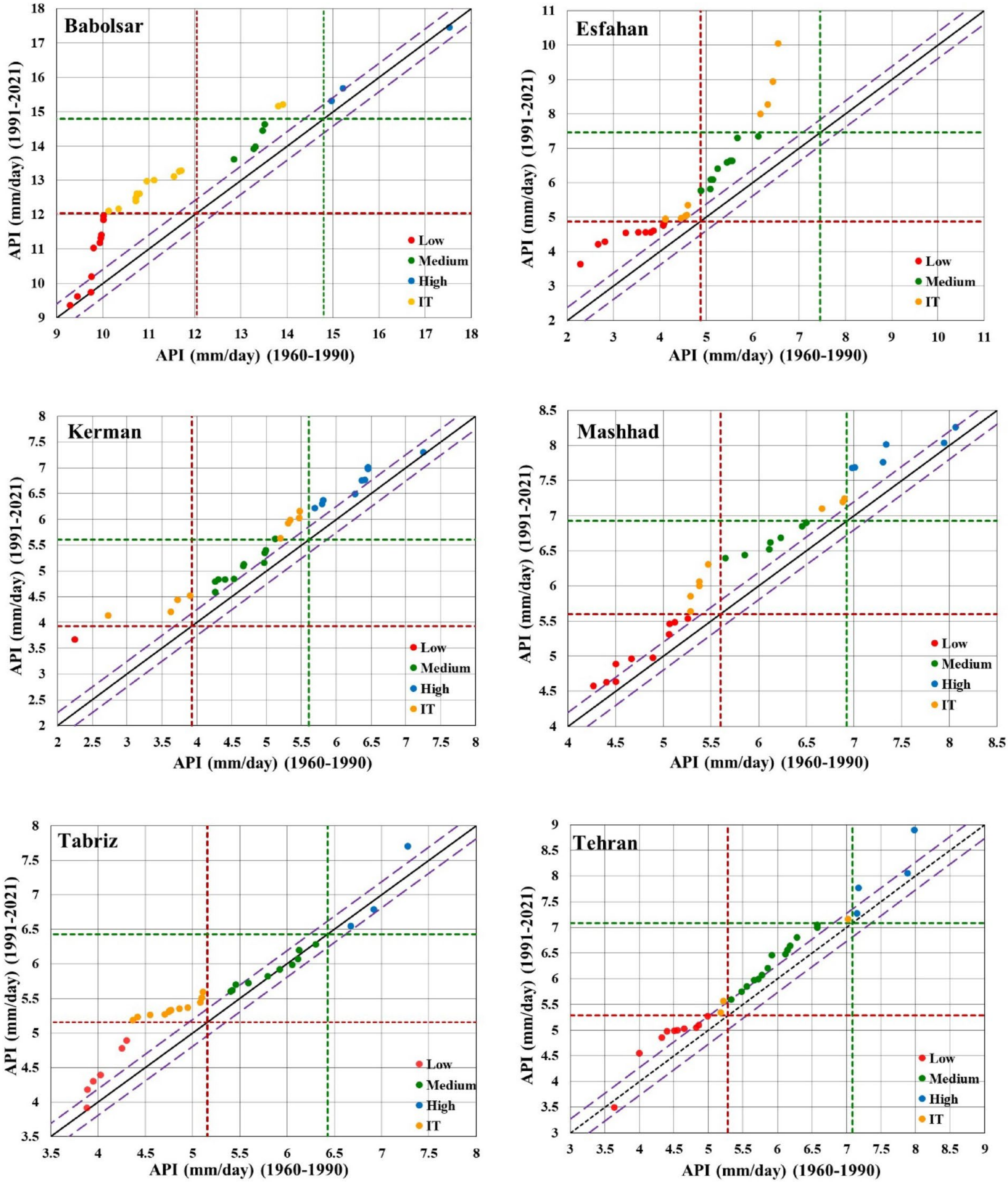

Fig. 7. The graphs of FITA method for API indicator.

Station	Range		TC	Grow percent			Total grow percent (TGP)
	I_{max}	I_{min}		low	Medium	High	
Babolsar	17.54	9.30	2.74	**16.64**	**11.55**	2.70	**14.14**
Esfahan	10.04	2.30	2.58	**11.28**	**18.30**	0.00	**14.68**
Kerman	7.29	2.26	1.68	**18.54**	**8.89**	**8.04**	**10.17**
Mashhad	8.25	4.27	1.33	**9.34**	**11.18**	**11.43**	**10.34**
Tabriz	7.70	3.89	1.27	**12.65**	1.58	1.18	**7.97**
Tehran	8.89	3.48	1.80	**5.95**	**6.29**	**8.03**	**6.38**

Table 6. Power of multi-level trend analysis in API index detected by FITA method for each level and all data. *Bold values are significant trends at the confidence level of 95%.

Climate index	Station	M-K	Sen slope	ITA		FITA
		Z	SS	D	S (CL 95%)	TGP
AT_{max}	Babolsar	**2.810**	0.031	0.161	**0.018** (0.004)	**5.581**
	Esfahan	**3.920**	0.028	0.311	**0.040** (0.003)	**23.697**
	Kerman	**4.280**	0.028	0.295	**0.037**(0.002)	**23.097**
	Mashhad	**3.460**	0.037	0.369	**0.047** (0.003)	**23.361**
	Tabriz	1.61	0.018	0.075	**0.009** (0.003)	4.536
	Tehran	1.34	0.006	0.073	**0.010** (0.002)	**7.419**
AT_{min}	Babolsar	**4.290**	0.055	**−9.135**	**0.055** (0.003)	**17.380**
	Esfahan	1.36	0.017	0.183	**−0.005** (0.005)	−1.112
	Kerman	**2.710**	0.054	−1.747	**0.082** (0.007)	**11.598**
	Mashhad	**4.530**	0.173	**−3.687**	**0.208** (0.007)	**27.612**
	Tabriz	**1.980**	0.054	−1.415	**0.072** (0.006)	**11.161**
	Tehran	**3.560**	0.073	**−3.117**	**0.082** (0.004)	**19.042**
APT	Babolsar	1.090	1.564	0.334	**0.947** (0.215)	3.498
	Esfahan	1.790	0.616	**2.076**	**0.734** (0.102)	**10.851**
	Kerman	**−2.280**	−0.754	−0.955	**−0.438** (0.062)	**−6.107**
	Mashhad	−0.085	−0.066	−0.503	**−0.411** (0.107)	−3.597
	Tabriz	**−2.260**	−1.278	−1.537	**−1.520** (0.082)	**−11.795**
	Tehran	0.810	0.532	0.658	**0.483** (0.079)	4.462
API	Babolsar	**2.903**	0.042	1.001	**0.038** (0.004)	**14.143**
	Esfahan	**3.190**	0.029	**2.428**	**0.037** (0.004)	**14.678**
	Kerman	1.450	0.012	1.008	**0.017** (0.002)	**10.172**
	Mashhad	**1.895**	0.015	0.699	**0.013** (0.001)	**10.339**
	Tabriz	1.430	0.010	0.584	**0.010** (0.002)	**7.969**
	Tehran	1.28	0.011	0.609	**0.011** (0.001)	**6.384**

Table 7. Comparison of the results of Mann-Kendal, sen's slope, ITA (D and S indicators), and FITA tests for the climate indices. *Bold values are significant trends at the confidence level of 95%.

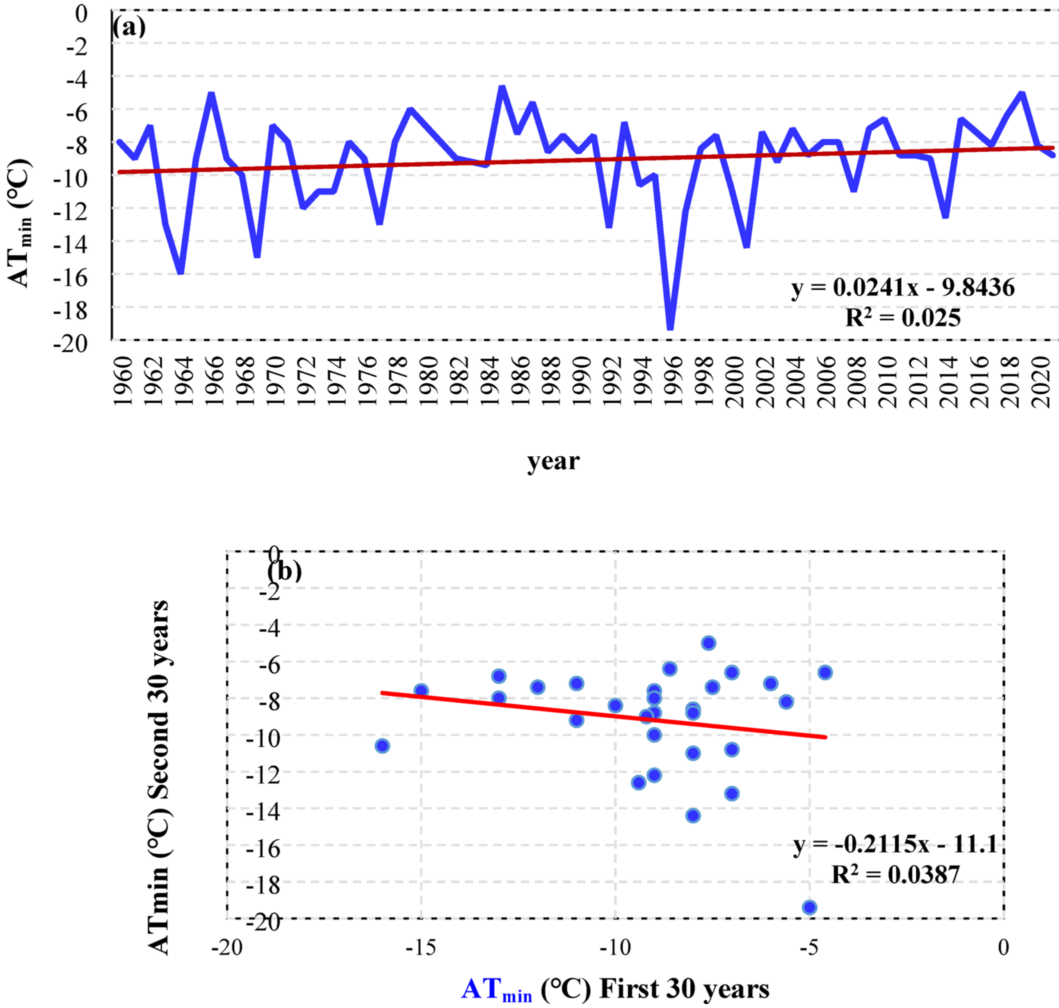

Fig. 8. Assessing the trend in the AT_{min} index at Esfahan station based on regression test for (a) all sequential data and (b) the second 30 years compared to the first 30 years.

Data availability

The datasets generated during and/or analyzed during the current study are available from the corresponding author on reasonable request.

Received: 17 May 2025; Accepted: 22 July 2025
Published online: 28 July 2025

References

1. Lee, H. et al. Climate Change 2023: Synthesis Report. Contribution of Working Groups I, II and III to the Sixth Assessment Report of the Intergovernmental Panel on Climate Change. (2023).
2. Danandeh Mehr, A. & Kahya, E. Climate change impacts on catchment-scale extreme rainfall variability: case study of Rize province, Turkey. *J. Hydrol. Eng.* **22**, 05016037 (2017).
3. Tabari, H. Climate change impact on flood and extreme precipitation increases with water availability. *Sci. Rep.* **10**, 13768 (2020).
4. Meresa, H., Tischbein, B. & Mekonnen, T. Climate change impact on extreme precipitation and peak flood magnitude and frequency: observations from CMIP6 and hydrological models. *Nat. Hazards*. **111**, 2649–2679 (2022).
5. Lucas, E. W. M. et al. Trends in climate extreme indices assessed in the Xingu river basin-Brazilian Amazon. *Weather Clim. Extremes*. **31**, 100306 (2021).
6. Alexander, L. V. et al. Global observed changes in daily climate extremes of temperature and precipitation. *J Geophys. Res Atmos* https://doi.org/10.1029/2005JD006290 (2006).
7. de los Skansi, M. Warming and wetting signals emerging from analysis of changes in climate extreme indices over South America. *Glob. Planet Change*. **100**, 295–307 (2013).
8. Keggenhoff, I., Elizbarashvili, M., Amiri-Farahani, A. & King, L. Trends in daily temperature and precipitation extremes over georgia, 1971–2010. *Weather Clim. Extremes*. **4**, 75–85 (2014).
9. Caloiero, T., Coscarelli, R., Ferrari, E. & Sirangelo, B. Trend analysis of monthly mean values and extreme indices of daily temperature in a region of Southern Italy. *Int. J. Climatol.* **37**, 284–297 (2017).
10. Attogouinon, A., Lawin, A. E., N'Tcha, M. & Houngue, R. Extreme precipitation indices trend assessment over the upper Oueme river Valley-(Benin). *Hydrology* **4**, 36 (2017).

11. Hong, Y. & Ying, S. Characteristics of extreme temperature and precipitation in China in 2017 based on ETCCDI indices. *Adv. Clim. Change Res.* **9**, 218–226 (2018).
12. Barry, A. et al. West Africa climate extremes and climate change indices. *Int. J. Climatol.* **38**, e921–e938 (2018).
13. Adeyeri, O., Lawin, A., Laux, P., Ishola, K. & Ige, S. Analysis of climate extreme indices over the Komadugu-Yobe basin, lake Chad region: past and future occurrences. *Weather Clim. Extremes*. **23**, 100194 (2019).
14. Bhatti, A. S. et al. Trend in extreme precipitation indices based on long term in situ precipitation records over Pakistan. *Water* **12**, 797 (2020).
15. Patra, P. & Satpati, L. Characteristics and trend analysis of absolute and relative temperature extremes indices and related indices of Kolkata. *Theoret. Appl. Climatol.* **148**, 943–954 (2022).
16. Güçlü, Y. S., Acar, R. & Saplıoğlu, K. Seasonally adjusted periodic time series for Mann-Kendall trend test. *Phys. Chem. Earth Parts A/B/C.* **138**, 103848 (2025).
17. Zhang, X. et al. Trends in Middle East climate extreme indices from 1950 to 2003. *J Geophys Res Atmos* https://doi.org/10.1029/2005JD006181 (2005).
18. Rahimi, M., Mohammadian, N., Vanashi, A. R. & Whan, K. Trends in indices of extreme temperature and precipitation in Iran over the period 1960–2014. *Open. J. Ecol.* **8**, 396 (2018).
19. Alavinia, S. H. & Zarei, M. Analysis of Spatial changes of extreme precipitation and temperature in Iran over a 50-year period. *Int. J. Climatol.* **41**, E2269–E2289 (2021).
20. Rahimi, M. & Hejabi, S. Spatial and Temporal analysis of trends in extreme temperature indices in Iran over the period 1960–2014. *Int. J. Climatol.* **38**, 272–282 (2018).
21. Ghiami-Shamami, F., Sabziparvar, A. A. & Shinoda, S. Long-term comparison of the climate extremes variability in different climate types located in coastal and inland regions of Iran. *Theoret. Appl. Climatol.* **136**, 875–897 (2019).
22. Soltani, M. et al. Assessment of climate variations in temperature and precipitation extreme events over Iran. *Theoret. Appl. Climatol.* **126**, 775–795 (2016).
23. Fathian, F. et al. Assessment of changes in climate extremes of temperature and precipitation over Iran. *Theoret. Appl. Climatol.* **141**, 1119–1133 (2020).
24. Chaparinia, F., Hadei, M., Yaghmaeian, K., Hadi, M. & Naddafi, K. Evaluation of climate indices related to water resources in Iran over the past 3 decades. *Sci. Rep.* **15**, 11846 (2025).
25. Kamali, S., Fattahi, E. & Habibi, M. Investigating the trend changes in temperature extreme indices in Iran. *Atmosphere* **16**, 483 (2025).
26. Rahimzadeh, F., Asgari, A. & Fattahi, E. Variability of extreme temperature and precipitation in Iran during recent decades. *Int. J. Climatology: J. Royal Meteorological Soc.* **29**, 329–343 (2009).
27. Rahimi, M. & Fatemi, S. S. Mean versus extreme precipitation trends in Iran over the period 1960–2017. *Pure. Appl. Geophys.* **176**, 3717–3735 (2019).
28. Şen, Z. Trend identification simulation and application. *J. Hydrol. Eng.* **19**, 635–642 (2014).
29. Rehman, S. Long-term wind speed analysis and detection of its trends using Mann–Kendall test and linear regression method. *Arab. J. Sci. Eng.* **38**, 421–437 (2013).
30. Amirataee, B. & Zeinalzadeh, K. Trends analysis of quantitative and qualitative changes in groundwater with considering the autocorrelation coefficients in West of lake Urmia, Iran. *Environ. Earth Sci.* **75**, 1–10 (2016).
31. Chervenkov, H. & Slavov, K. Theil-Sen estimator vs. ordinary least squares–trend analysis for selected ETCCDI climate indices. *Comptes Rendus Acad. Bulg. Sci.* **72**, 47–54 (2019).
32. Şen, Z. Innovative trend analysis methodology. *J. Hydrol. Eng.* **17**, 1042–1046 (2012).
33. Kişi, Ö., Santos, C. A. G., da Silva, R. M. & Zounemat-Kermani, M. Trend analysis of monthly streamflows using şen's innovative trend method. *G Eofizika*. **35** (68-), 53 (2018).
34. Gumus, V., Avsaroglu, Y. & Simsek, O. Streamflow trends in the Tigris river basin using Mann – Kendall and innovative trend analysis methods. *J. Earth Syst. Sci.* **131**, 34 (2022).
35. Kuriqi, A. et al. Seasonality shift and streamflow variability trends in central India. *Acta Geophys.* **68**, 1–15. https://doi.org/10.1007/s11600-020-00475-4 (2020).
36. Caloiero, T., Coscarelli, R. & Ferrari, E. Assessment of seasonal and annual rainfall trend in Calabria (southern Italy) with the ITA method. *J. Hydroinformatics*. **22**, 738–748 (2020).
37. Nisansala, W., Abeysingha, N., Islam, A. & Bandara, A. Recent rainfall trend over Sri Lanka (1987–2017). *Int. J. Climatol.* **40**, 3417–3435 (2020).
38. Danandeh Mehr, A., Hrnjica, B., Bonacci, O. & Torabi Haghighi, A. Innovative and successive average trend analysis of temperature and precipitation in osijek, Croatia. *Theoret. Appl. Climatol.* **145**, 875–890. https://doi.org/10.1007/s00704-021-03672-3 (2021).
39. Tosunoglu, F. & Kisi, O. Trend analysis of maximum hydrologic drought variables using Mann–Kendall and şen's innovative trend method. *River Res. Appl.* **33**, 597–610. https://doi.org/10.1002/rra.3106 (2017).
40. Wu, H. & Qian, H. Innovative trend analysis of annual and seasonal rainfall and extreme values in shaanxi, china, since the 1950s. *Int. J. Climatol.* **37**, 2582–2592 (2017).
41. Wang, Y. et al. Innovative trend analysis of annual and seasonal rainfall in the Yangtze river delta, Eastern China. *Atmos. Res.* **231**, 104673 (2020).
42. Zerouali, B. et al. Improving the visualization of rainfall trends using various innovative trend methodologies with time–frequency-based methods. *Appl. Water Sci.* **12**, 207. https://doi.org/10.1007/s13201-022-01722-3 (2022).
43. Güçlü, Y. S. Trend stability identification by three-dimensional model. *Model. Earth Syst. Environ.* **8**, 4333–4340 (2022).
44. Demirel, İH., Kesgin, E., Güçlü, Y. S., Tan, R. İ & Başaran, B. Trend stability assessment for hydrological drought in Euphrates Basin (Türkiye) using triple wilcoxon test and innovative trend analysis methods. *Water* https://doi.org/10.3390/w16192823 (2024).
45. Cui, L. et al. Innovative trend analysis of annual and seasonal air temperature and rainfall in the Yangtze river basin, China during 1960–2015. *J. Atmos. Solar Terr. Phys.* **164**, 48–59 (2017).
46. Şen, Z. Innovative trend significance test and applications. *Theoret. Appl. Climatol.* **127**, 939–947. https://doi.org/10.1007/s00704-015-1681-x (2017).
47. Saplıoğlu, K. & Güçlü, Y. S. Combination of Wilcoxon test and scatter diagram for trend analysis of hydrological data. *J. Hydrol.* **612**, 128132 (2022).
48. Modaresi, F. & Araghi, A. Projecting future reference evapotranspiration in Iran based on CMIP6 multi-model ensemble. *Theoretical Appl Climatology* **153**, 1–12 (2023).
49. Janarthanan, R., Balamurali, R., Annapoorani, A. & Vimala, V. Prediction of rainfall using fuzzy logic. *Mater Today Proc* **37**, 959–963. https://doi.org/10.1016/j.matpr.2020.06.179 (2021).
50. Asklany, S. A., Elhelow, K. & Youssef, I. K. Abd El-wahab, M. Rainfall events prediction using rule-based fuzzy inference system. *Atmos. Res.* **101**, 228–236. https://doi.org/10.1016/j.atmosres.2011.02.015 (2011).
51. Marzano, F. S., Scaranari, D. & Vulpiani, G. Supervised Fuzzy-Logic classification of hydrometeors using C-Band weather radars. *IEEE Trans. Geosci. Remote Sens.* **45**, 3784–3799. https://doi.org/10.1109/TGRS.2007.903399 (2007).
52. Tayfur, G. & Brocca, L. Fuzzy logic for Rainfall-Runoff modelling considering soil moisture. *Water Resour. Manage.* **29**, 3519–3533. https://doi.org/10.1007/s11269-015-1012-0 (2015).

53. Danandeh Mehr, A., Tur, R., Çalışkan, C. & Tas, E. A. Novel fuzzy random forest model for meteorological drought classification and prediction in ungauged catchments. *Pure. Appl. Geophys.* **177**, 5993–6006. https://doi.org/10.1007/s00024-020-02609-7 (2020).
54. Kisi, O. An innovative method for trend analysis of monthly Pan evaporations. *J. Hydrol.* **527**, 1123–1129. https://doi.org/10.1016/j.jhydrol.2015.06.009 (2015).
55. Mann, H. B. Nonparametric tests against trend. *Econometrica J. econom soc* **13**, 245–259 (1945).
56. Kendall, M. *Rank Correlation Methods 4th edn* (Charles Griffin, 1975).
57. Partal, T. & Kahya, E. Trend analysis in Turkish precipitation data. *Hydrol. Processes: Int. J.* **20**, 2011–2026 (2006).
58. Sen, P. K. Estimates of the regression coefficient based on kendall's Tau. *J. Am. Stat. Assoc.* **63**, 1379–1389 (1968).
59. Nourani, V., Danandeh Mehr, A. & Azad, N. Trend analysis of hydroclimatological variables in urmia lake basin using hybrid wavelet Mann–Kendall and Şen tests. *Environ. Earth Sci.* **77**, 1–18 (2018).
60. Dabanli, I., Şişman, E., Güçlü, Y. S., Birpınar, M. E. & Şen, Z. Climate change impacts on sea surface temperature (SST) trend around Turkey seashores. *Acta Geophys.* **69**, 295–305 (2021).
61. Amirataee, B. & Zeinalzadeh, K. Trends analysis of quantitative and qualitative changes in groundwater with considering the autocorrelation coefficients in West of lake urmia, Iran. *Environ. Earth Sci.* **75**, 371. https://doi.org/10.1007/s12665-015-4917-2 (2016).
62. Kisi, O. & Ay, M. Comparison of Mann–Kendall and innovative trend method for water quality parameters of the Kizilirmak river, Turkey. *J. Hydrol.* **513**, 362–375. https://doi.org/10.1016/j.jhydrol.2014.03.005 (2014).
63. Dabanlı, İ. et al. Trend assessment by the Innovative-Şen method. *Water Resour. Manage.* **30**, 5193–5203. https://doi.org/10.1007/s11269-016-1478-4 (2016).

Acknowledgements
The authors are grateful to the Iran Meteorological Organization for providing data as well as Ferdowsi University of Mashhad (FUM) for supporting this research.

Author contributions
Conceptualization, F.M. and A.D.M.; methodology, F.M. and A.D.M.; software, F.M. and I.S.B.; validation, M. J.S.S., F.M. and A.D.M.; formal analysis, F.M. and I.S.B.; investigation, A.D.M. and F.M.; resources, A.D.M. and F.M.; data curation, F.M.; writing—original draft preparation, F.M. and A.D.M.; writing—review and editing, M. J.S.S., F.M. and A.D.M.; visualization, F.M.; supervision, F.M. All authors have read and agreed to the published version of the manuscript.

Declarations

Competing interests
The authors declare no competing interests.

Additional information
Correspondence and requests for materials should be addressed to F.M.